JOURNAL OF MATERIALS SCIENCE **34** (1999) 2377–2387

The effects of deforming knitted glass fabrics on the basic composite mechanical properties

K. H. LEONG*
Cooperative Research Centre for Advanced Composite Structures Ltd (CRC-ACS), 506 Lorimer Street, Fishermens Bend, VIC 3207, Australia
E-mail: khlcrcas@ozemail.com.au

M. NGUYEN, I. HERSZBERG
The Sir Lawrence Wackett Centre for Aerospace Design and Technology, Royal Melbourne Institute of Technology (RMIT), GPO Box 2476V, Melbourne, VIC 3001, Australia

The effects of deforming knitted fabrics on the tensile and compressive properties of their composites have been investigated for the weft-knit Milano rib fibre architecture. The properties have been studied for both the course and wale directions for composites with fabrics deformed in either of the two directions. It was found that any change in the mechanical properties of the deformed composites with respect to their undeformed counterpart is strongly related to the changes in the knit structure brought about by the induced deformation to the knitted fabric. Deformation in the knitted fabric also affects the tensile fracture mode whereby increased deformation, be it wale- or course-wise, transforms transverse fracture to shear fracture in either loading axis. On the contrary, the compressive fracture mode is insensitive to fabric deformation. Fractographic studies using stereo-optical and scanning electron microscopy have further revealed that tensile failure is caused by fibre breakages occurring at two locations of the knitted loops—one, at the leg components and, two, at fibre crossover points, whilst compression failure is controlled by Euler buckling of the looped fibres of the knitted composite. All these characteristics were revealed to be related to the microstructure of the knitted composite laminates.

1. Introduction

Polymer composite structures with complex shapes can be difficult and expensive to manufacture using standard prepreg or wet lay-up technology due to the lack of formability, the requirement for skilled workers and the labour-intensive nature of these more conventional processes. Over the years, the textile manufacturing industry has developed the ability to produce near-net-shape fabrics with a three-dimensional fibre network using highly automated techniques such as stitching, weaving, braiding and knitting. The use of this technology with advanced fibres such as glass, carbon and aramid, and suitable liquid moulding techniques such as resin film infusion (RFI) or resin transfer moulding (RTM), has been shown to possess tremendous potential for lowering the manufacturing cost of composite structures.

Amongst the various textile techniques, knitting is probably one of the more suitable methods for manufacturing intricately shaped composite structures. The use of advanced knitting machines allows the production of near-net-shape preforms including T-pipe junctions, cones, flanged pipes and domes [1, 2]. Whilst such preforms are obviously advantageous in shaving production cost by minimising material wastage and reducing labour time, the development of a suitable preform which conforms to prerequisite properties can be a time consuming and, hence, expensive task. The exercise of deforming a piece of flat knitted fabric over a shaped tool appears to be a good alternative. During the process of forming a flat knitted fabric (e.g. during deep drawing), it is inevitable that the fabric would be deformed due to stretching so that optimum conformibility to the shape of the component is achieved. The highly looped fibre architecture of the knitted fabric easily affords such deformation, and, hence, its excellent forming characteristics. However, stretching the fabric results in distortion to the knit structure which could result in tearing and/or isolated bunching of the fabric [3]. Deformation to the fabric could also cause a degree of fibre orientation in the direction of stretch that would, in turn, affect the mechanical properties of the knitted composite [4, 5]. In the present study, the effects of deforming knitted fabrics on the tensile and compressive properties of their composites have been investigated for the weft-knit Milano rib fibre

* Author to whom all correspondence should be addressed.

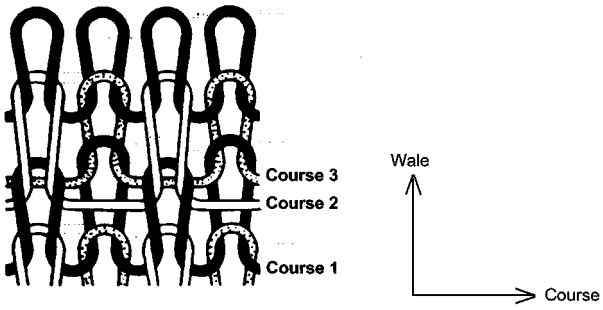

Figure 1 Schematic of the Milano rib structure.

architecture. The properties have been studied for both the course and wale directions for composites with fabrics deformed in either of the two directions. Fractographic studies using stereo-optical and scanning electron microscopy have also been carried out to investigate the fracture mechanisms operating in the composites under the two different loading conditions.

2. Experimental

2.1. Materials

The test panels used in this study were manufactured via RTM from up to 7 layers of weft-knit Milano rib fabric (see Fig. 1 for loop structure) and Derakane 411-C50 vinyl ester resin. The resin was used in conjunction

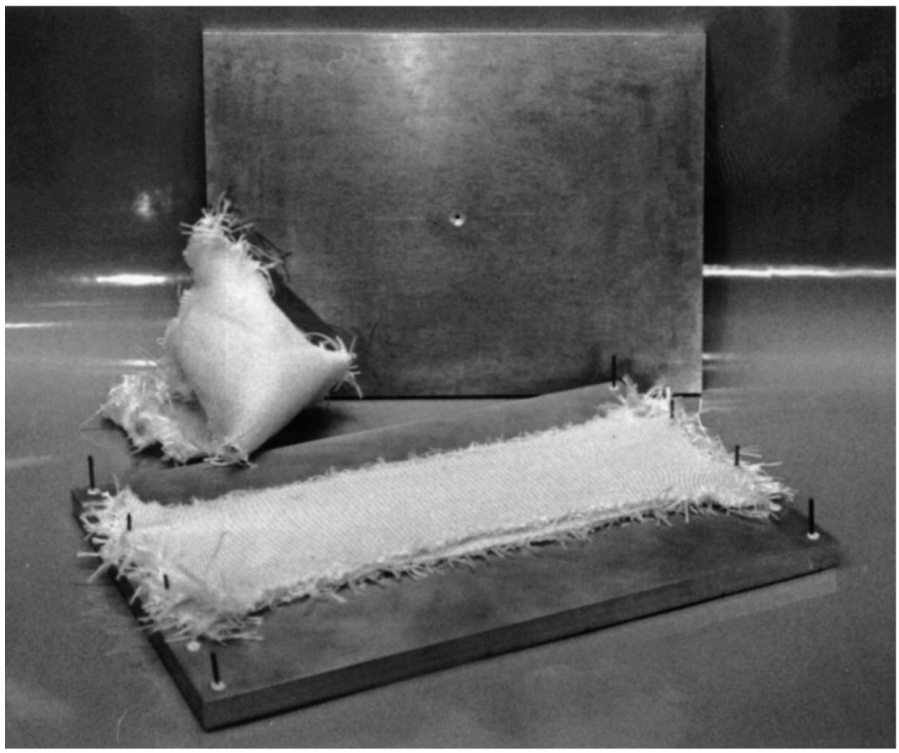

(a)

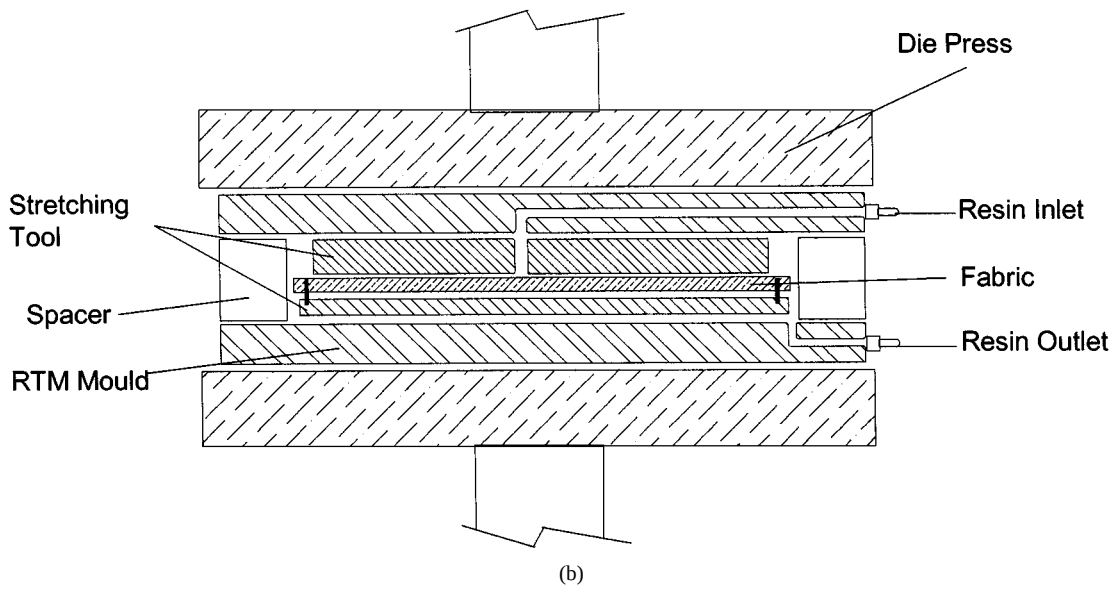

(b)

Figure 2 RTM tooling used to manufacture the knitted composite laminates. (a) Rig used to deform the fabric prior to consolidation. (b) Schematic of the RTM tooling used to produced the test panels.

with 2.0% Triganox T-239 (catalyst), 0.5% Conap (promoter) and 0.05% 2,4-P (inhibitor). A 10-gauge flat bed weft knitting machine was employed to produce a (undeformed) fabric with nominal areal weight of 730 g m^{-2} using 2 × 68 tex multi-filament glass fibre. In each complete repeat of the Milano rib structure, it consists of three courses—two rows of single jerseys, that are knitted on two separate set of needles, which are held together by a row of 1 × 1 rib. Consequently, the resultant fabric is balanced, i.e. the face and back surfaces are identical in construction and, hence, appearance.

2.2. Manufacture

Fabrics were deformed to 20, 35 and 45% (maximum achievable) in the course direction and 20, 30 and 40% (maximum achievable) in the wale direction. Undeformed (0%) fabrics were also considered in this study and they were used as reference materials. The two maximum achievable deformation states were determined experimentally as the point at which the fabric begins to fray at the edges under the influence of stretching. The fibre volume fractions (V_f) of the knitted composite laminates were maintained fairly constant at approximately 55% by varying the number of knitted fabric layers so as to isolate the effect of fibre content on strength and stiffness. Furthermore, a reasonably uniform resin flow pattern and, hence, quality in terms of porosity and wetting between the different laminates could also be maintained. The laminates were subsequently manufactured using either 6 or 7 layers of fabric.

All the fabrics were deformed in tension to the required amount in a purpose-built rig [6] (see Fig. 2a) by stretching cut-to-size pieces of fabric and pinning it down at the edges of the tool. This process was carried out prior to resin impregnation during which the rig was incorporated into an existing RTM mould (see Fig. 2b). To consolidate the knitted fabric a pressure pot system was used to inject the resin through an inlet port. When resin was detected at the outlet port, inlet pressure and outlet vacuum were sealed and the composite was allowed to consolidate under clamping pressures at a cure temperature of 80 °C for 4 hours. The test panels were then postcured for a further 2 hours at 120 °C. Spacers were used in the tool to ensure that the required nominal sample thickness of 3 mm was obtained. It should however be noted that the cured thickness of the test panels and the areal weight of the fabric do actually deviate somewhat from nominal values so that slight variations in fibre content were recorded for the test panels of the same type.

2.3. Mechanical tests

Tension tests were carried out on straight-sided samples measuring nominally 25 mm by 220 mm at a displacement rate of 0.5 mm min^{-1} using a 50 kN MTS screw-driven testing machine. A gauge length of 130 mm was used and up to 6 samples were considered for each case. For the compression tests, straight-sided samples of 25 mm by 56 mm nominal dimensions were loaded

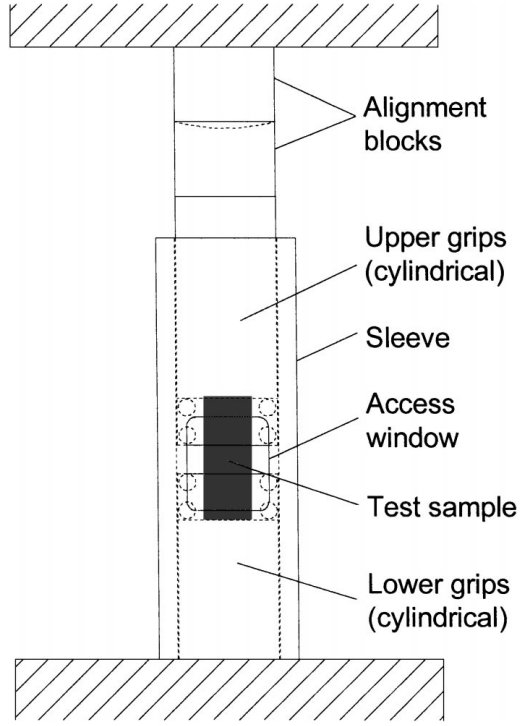

Figure 3 Schematic diagram of the compression test rig used for the present work.

at a displacement rate of 0.5 mm min^{-1} in a modified Celanese/IITRI test rig (see Fig. 3) using a 100 kN Instron servo-hydraulic testing machine. A gauge length of 6 mm was used and no less than 5 samples were tested for each condition.

An open mesh emery cloth (Screenbak^{TM}) was used in the gripped areas of the samples instead of end tabs for all the tests and this appeared to be effective in ensuring failure within the gauge length. For both the tension and compression tests, samples were tested along the wale as well as the course axes. To identify each test condition, a notation system containing two consecutive alphabets, which represents the directions of deformation and loading, respectively, and a numeric, the degree of deformation, is used in this paper. For instance, '45WC' represents a sample made from a fabric that has undergone 45% deformation in the wale direction and tested along the course axis.

3. Results

3.1. Stress-strain behaviours

The typical tensile stress-strain behaviour for the knitted composite is illustrated in Fig. 4. The composite basically exhibits linear behaviour at the early stages of loading but very quickly transforms to pseudo-plastic before reaching a maximum stress (defined as the tensile strength of the composite) followed by a sharp drop in stress.

Fig. 5 shows a typical compressive stress-strain curve for the knitted composite, plotted alongside its out-of-plane deflection history. The graph reveals that, as in the case of tensile loading, the composite initially exhibites elastic behaviour and then transforms to pseudo-plastic before reaching a maximum stress (defined as the compressive strength of the composite), after which a

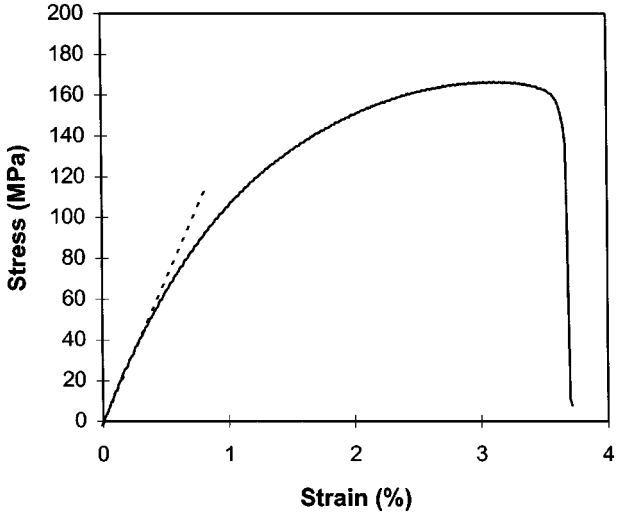

Figure 4 Typical tensile stress-strain curve of the knitted composites.

steep reduction in stress ensues. It should be noted that despite an early onset, the compression samples exhibit only a negligible amount of out-of-plane buckling until the point of final failure.

In both the tensile and compressive loading conditions, the stress-strain behaviours of the knitted composite are independent of loading axis and the direction and amount of deformation in the fabric.

3.2. Microstructures

Fig. 6 illustrates the effect of deformation on the Milano rib knit structure under both the wale and course deformed conditions. It will be noticed that two distinct structural patterns emerge depending on the direction of stretch. Compared with the as-received, undeformed fabric, the wale deformed fabric appears to have extended leg components and smaller radii in the knitted loops, which, on the whole, also seem to have been drawn closer together. Despite these differences, the overall knit structure of the undeformed fabric is, by and large, retained even under heavy deformation (compare Fig. 6a with Figs. 6b and c).

On the contrary, the course deformed fabric exhibits a more ordered and block-like structure that is quite distinct from its undeformed counterpart, and this induced structure is enhanced as the degree of deformation is increased (compare Fig. 6a with Figs. 6d and e). This deformed structure results as rows of courses are drawn together, simultaneously causing columns of wales to move apart under the influence of stretching, thereby leaving a structure which is overall more open compared to its undeformed counterpart.

3.3. Mechanical properties

The influence of deformation on the tension and compression properties of the knitted composites is presented in Figs. 7 through 10. The fibre content of the different laminates varied between 52 and 57% and, therefore, to afford a comparison between them, the results presented in the four figures have been normalised to a constant V_f of 55%.

It will be noted from Figs. 7 and 8 that if the fabric were not deformed, the tensile strength and stiffness of the composite laminates are higher in the wale than in the course direction. When the fabric is deformed along the wale axis, both the strength and stiffness are improved regardless of the loading direction. Course deformation, however, only improves strength and stiffness along the stretch axis, but normal to that, the two properties are degraded.

Under compression loading, the strength of the undeformed composite laminates in the wale and course directions are virtually the same although stiffness in the wale direction appears to be somewhat higher. Wale deformation improves stiffness along both the wale and course directions but strength is only improved in the wale direction and degraded in the course direction. Deforming the fabric along the course axis appears to degrade compressive strength regardless of the loading

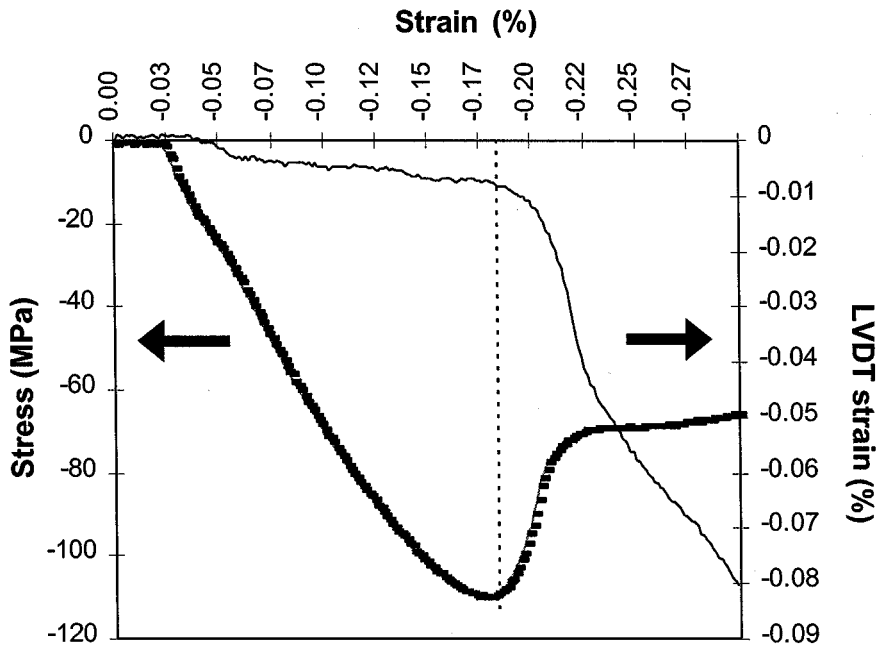

Figure 5 Typical compressive stress-strain curve of the knitted composites.

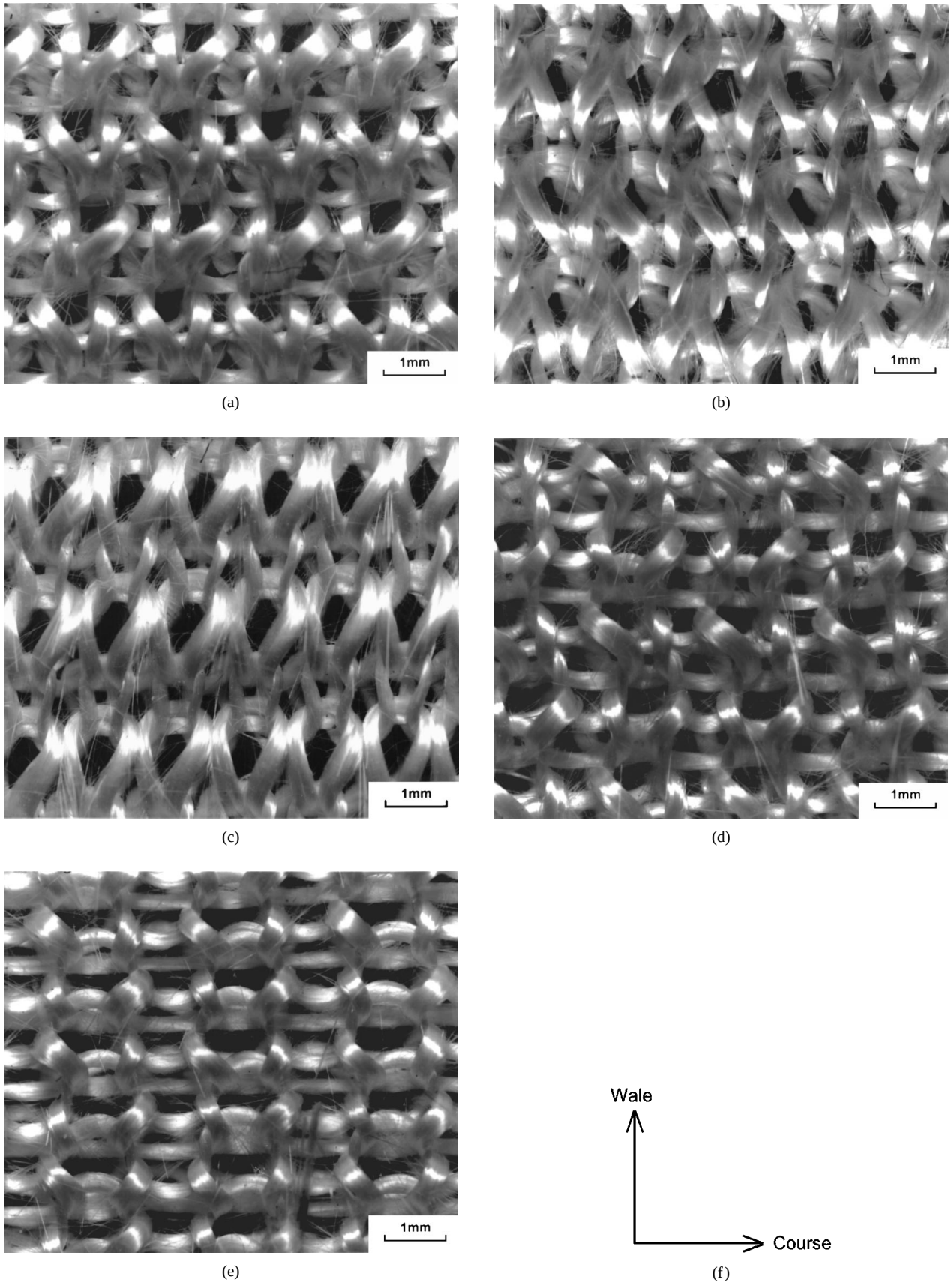

Figure 6 The effects of deformation on the effective fibre architecture of the Milano rib fabric. (a) Undeformed, As-received (0%). (b) Wale deformed, Light (10%). (c) Wale deformed, Heavy (30%). (d) Course deformed, Light (10%). (e) Course deformed, Heavy (30%).

axis, whilst stiffness is only slightly improved in the wale direction but remains virtually unaffected in the course direction. These results are represented graphically in Figs 9 and 10.

3.4. Fracture mechanisms

Regardless of the amount of deformation in the fabric or the loading direction, the first discernible damage in the tensile samples was observed to be matrix

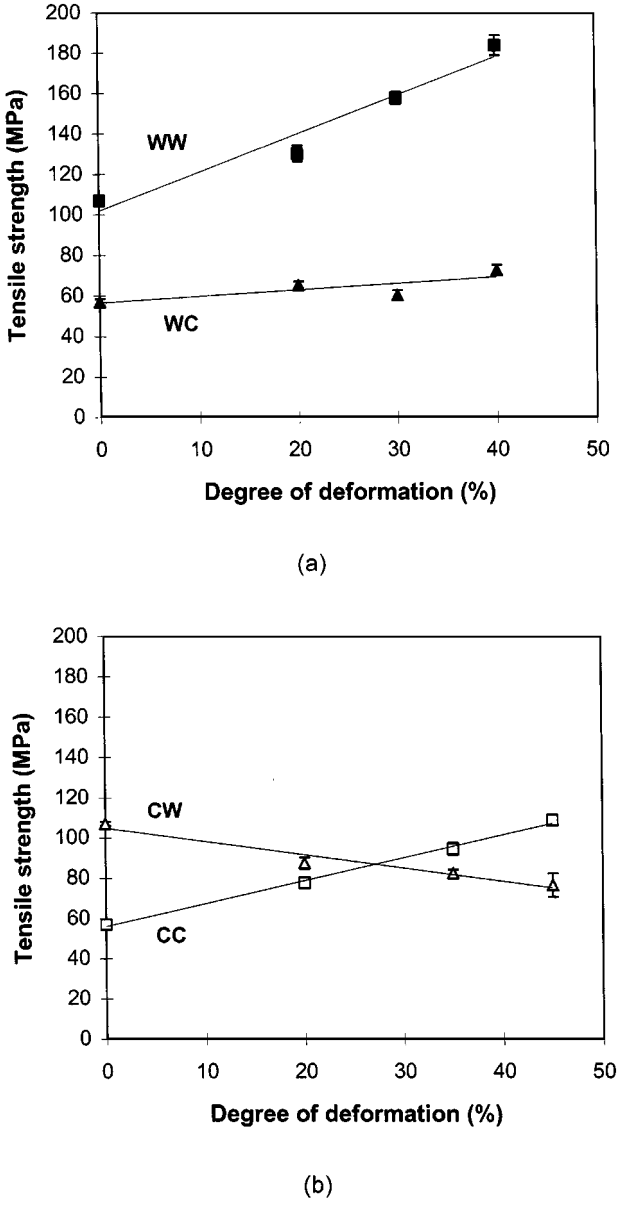

Figure 7 The influence of deformation of the knitted fabric on the composite tensile strength.

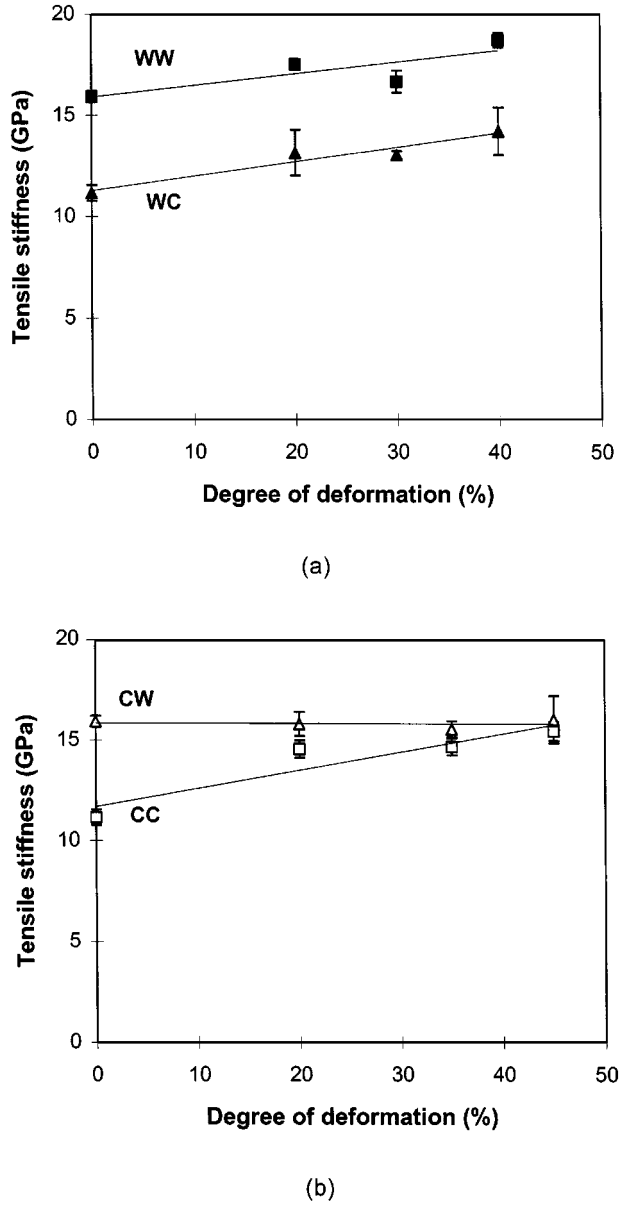

Figure 8 The influence of deformation of the knitted fabric on the composite tensile stiffness.

cracking (see Fig. 11). This microcracking, which coincides with the transition from linear to nonlinear stress-strain behaviour (see Fig. 4), appears macroscopically as whitened areas in the test samples which increases in intensity as loading progresses until final failure of the samples occurs. The locations of the microcracks within the gauge section are initially relatively random, but with increased loading the amount of microcracking multiplies and the microcracks appears to gradually coalesce, thence forming regular rows of matrix cracks that extend the whole width of the sample. Earlier work by Leong *et al.* [7] has revealed that these microcracks do not actually span the whole thickness of the laminates but are arrested by the complex array of fibres due to the heavy intermeshing between the different fabric layers. They also pointed out that the matrix crack spacings are of the order of the distances between the loop components in the fabric corresponding to the loading axis, and this observation appears to have been duplicated here for the present laminates.

In the present work, ultimate failure is defined as the point at which there was an appreciable drop in the load-carrying capacity of the test sample. In most cases when this happens, the samples are not completely broken but rather the matching fracture surfaces are bridged by a ligament of fabric material. Consistent with this fracture behaviour, ultimate failure of the test samples is not catastrophic. The appreciable drop in the load-carrying capacity, and, hence, ultimate failure of the samples, occurs with the onset of gross fibre fracture, i.e. breakage of the first significant group of fibre tows.

The amount of deformation in the fabric also has an influence on the tensile fracture mode. Fig. 11 shows that the knitted composites can fail in one of three modes with respect to the relative orientation of the fracture plane and the loading axis. Regardless of which direction the fabric had been stretched, the samples of undeformed (and lightly deformed) fabric fail in a plane normal to the loading axis (see Fig. 11a) whilst the

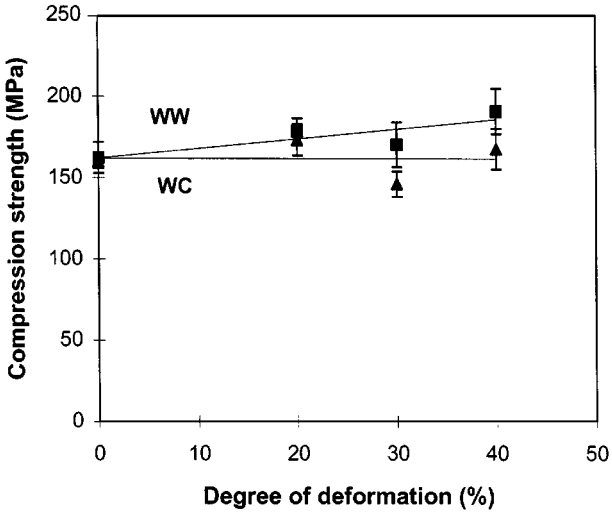

(a)

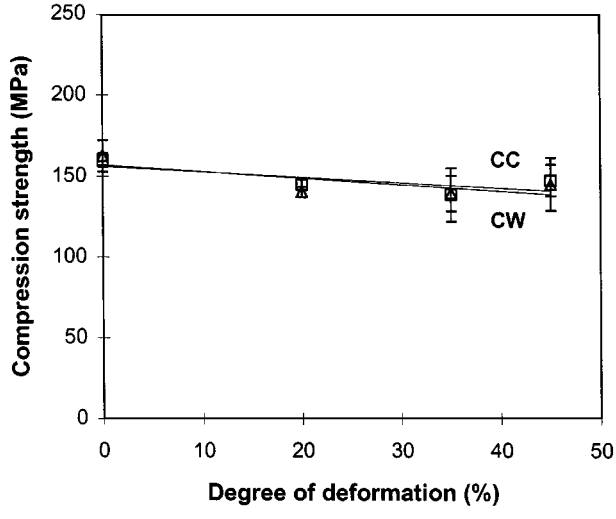

(b)

Figure 9 The influence of deformation of the knitted fabric on the composite compressive strength.

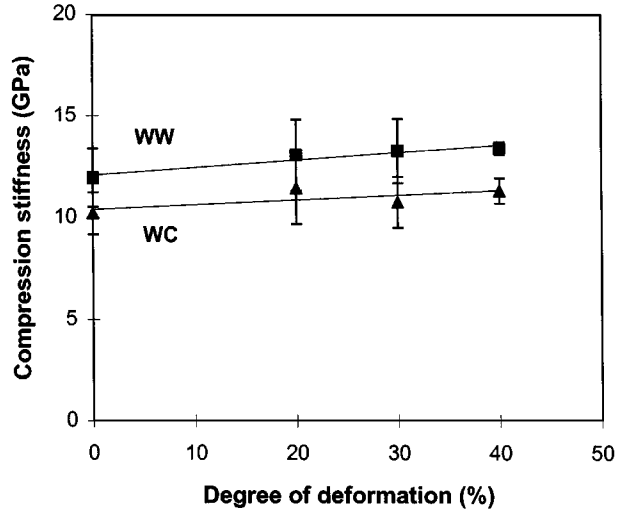

(a)

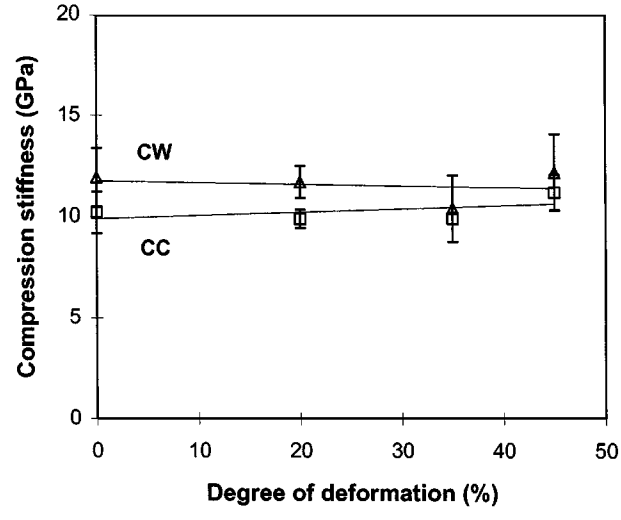

(b)

Figure 10 The influence of deformation of the knitted fabric on the composite compressive stiffness.

samples of more heavily deformed fabrics generally fail at an angled plane of approximately 20° to 30° (see Fig. 11c). It has been noted that the angles of the fracture planes on the whole increase with the amount of deformation in the fabrics. In some cases, the samples would fail in a combination of the two modes, usually initiating at an angle and finishing up normal, to the loading axis (see Fig. 11b).

Fig. 12 shows representative scanning electron micrographs of the tensile samples after failure. From Figs 12a, c and e it can be seen that fracture consistently occurs at two locations of the knitted loops, one, at the leg components and, two, at fibre crossover points. These sources of failure have been widely reported for a number of different knitted composites [8, 9], and they respectively coincide with cross-sections of minimum fibre content and regions of highly stressed fibres. These observations are common for all the laminates under investigation regardless of the loading axis and the amount of induced deformation in the fabric.

Optical and scanning electron microscopy reveals that compressive failure is by and large due to Euler buckling of fibre tows in the laminates, as exemplified in Fig. 13. The catalyst for this buckling is clearly the kink in the fibres which is a direct result of the looped fibre architecture that is typical of knit structures. The gross effect of these fibre breakages is shear failure of the compression test samples (see Fig. 14a). In most of the samples, however, shear failure is evident only on one edge of the samples while crushing appears to have taken place on the far edge (see Fig. 14b).

4. Discussion

The weft-knit Milano rib composite under investigation is anisotropic in tension. It is on the whole stronger and stiffer when loaded along the wale axis compared with along the course. Although no systematic measurements have been carried out, it is quite clear from qualitative assessments that the content of fibres

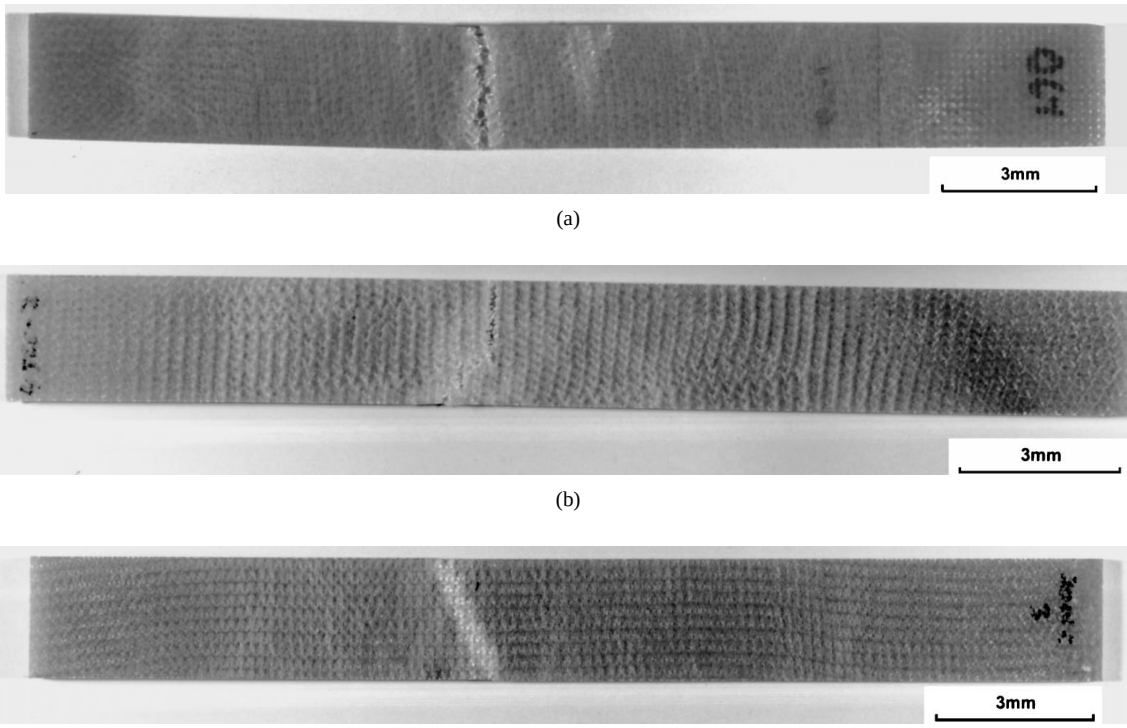

Figure 11 Examples of failed tensile samples of (a) undeformed, and (b and c) deformed, fabrics. (a) Undeformed, tested along the course axis; (b) 45CC; (c) 30WC.

oriented in the wale direction is higher, which would account for the superior tensile properties along that axis. The improvements in tensile properties with increased deformation are considerably more pronounced for strength (72.4% for 40WW and 89.9% for 45CC) than they are for stiffness (17.5% for 40WW and 38.5% for 45CC). This is not unexpected since a slight misalignment in fibre orientation from the loading axis (up to $\sim 25^{\circ}$) is known to have a more significant influence on strength than on stiffness. Under compression, on the other hand, due to the high dominance of the matrix properties, the laminates exhibit virtually similar strength and stiffness in the two principal loading axes.

When the knitted fabric is stretched, the overall distribution and orientation of the fibres are changed. In the present work it is evident that this could translate to a complete change of the knit structure depending on the direction of stretch, which in turn could have significant consequences on the tension and compression properties of the knitted composites. For wale deformed laminates, tensile strength (72.4% for 40WW and 12.0% for 40WC) and stiffness (17.5% for 40WW and 21.0% for 40WC) are improved with stretching irrespective of the loading axis. This is because as the fabric is stretched, as Figs 6a–c show, the fibres are increasingly drawn to the direction of stretch (thus improving fibre loading) and/or straightened (thus improving directionality) along both the wale and course axes.

The improved fibre loading and directionality also has a positive effect on compression strength (17.6% for 40WW) and stiffness (12.0% for 40WW) along the axis of stretch as the contribution of the fibres to mechanical properties becomes more significant and the dominance of the matrix starts to wane somewhat. The improvement in compressive strength along the course axis is, however, quite negligible (5.1% for 40WC) since fibre loading in that direction is expected to deteriorate as the fabric is stretched along the wale axis. Nevertheless, stiffness along the axis normal to fabric stretch is enhanced (10.8% for 40WC) and this is believed to be attributed to the improved fibre directionality due to stretching.

Deformation along the course axis results in an improvement and a degradation in both tensile strength (89.9% for 45CC and -35.8% for 45CW) and stiffness (38.5% for 45CC and -4.2% for 45CW) along and normal to the stretch axes, respectively. It can be seen from Figs 6a, d and e that stretching along the course axis results in very efficient straightening of the fibres and, hence, the improved course-wise properties. However, as course deformation is increased, the individual rows of courses are also at the same time drawn increasingly closer together as the individual columns of wales moves apart thereby effectively reducing the amount of fibres that contribute to the wale-wise properties. Consequently the wale-wise tensile properties are degraded.

The course deformed knit structure, which is quite distinct from its undeformed, as-received counterpart, however, brings about only a slight improvement in compressive stiffness regardless of the loading axis (9.8% for 45CC and 2.5% for 45CW). These superior stiffness values are almost certainly due to the enhanced directionality of the fibres, but, at the same time, because of the dominance of the matrix on compression properties, only small improvements are evident. Despite the fact that fibres in the course deformed

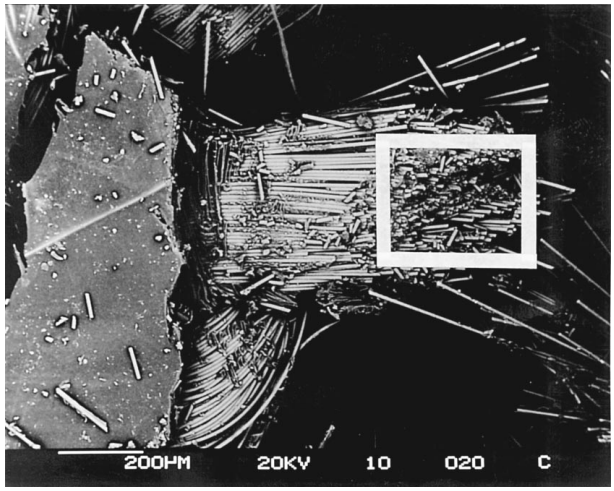

(a)

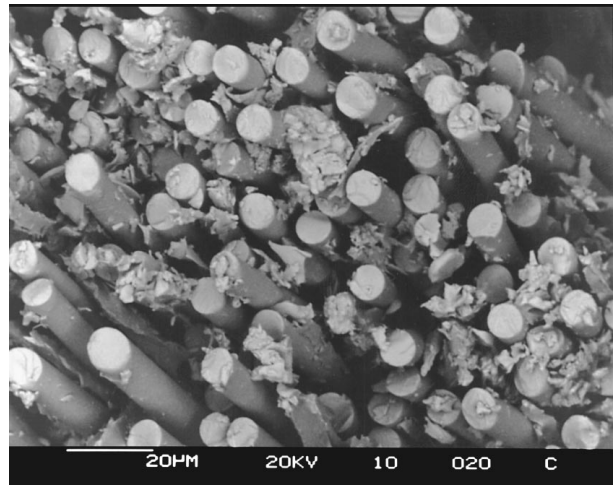

(b)

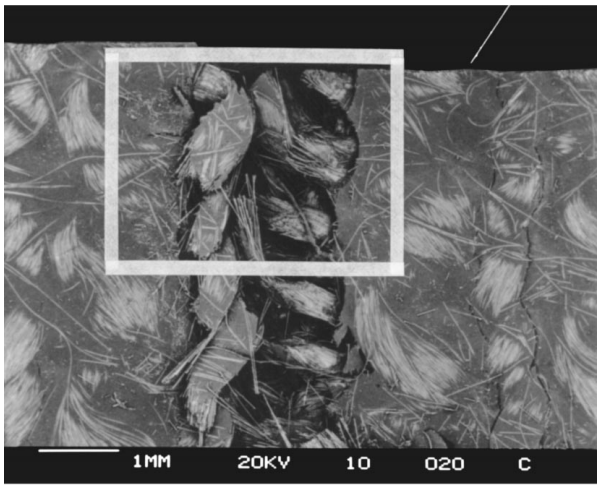

(c)

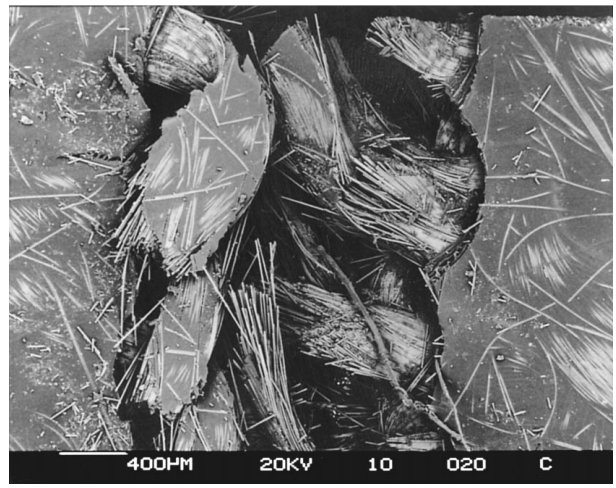

(d)

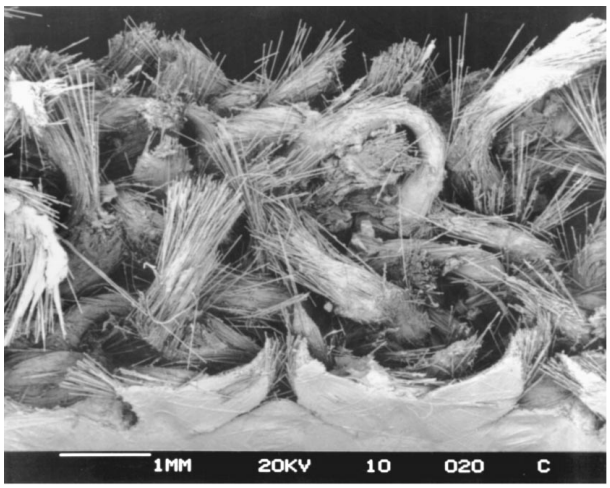

(e)

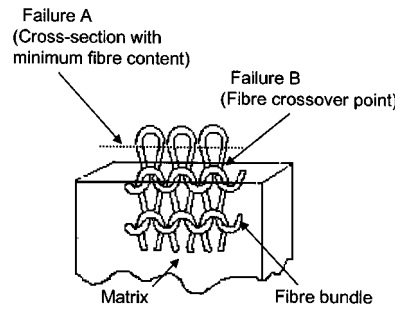

(f)

Figure 12 Representative scanning electron micrographs of tensile failure. (a) Fractured fibre tow at the region of lowest fibre content in the test sample. (b) Closeup of fibre tow in Fig. 12a showing brittle fracture in the fibres. (c) Fractured fibre tow at the fibre crossover points. (d) Closeup of the boxed region in Fig. 12c. (e) Fracture surface showing failure of fibre tows occurring in both the regions of lowest fibre content and fibre crossover points. (f) Schematic diagram showing possible failure locations under tensile loads.

structure have been significantly straightened, compression strength of the laminates are lower than their as-received counterpart (−7.6% for 45CC and −10.6 for 45CW). It is understood from fractographic studies that the strength of the knitted laminates in compression is dictated by Euler buckling in the fibres and because the course deformed structure appears to be more open (compare Fig. 6a with Figs 6d and e) it is probable that the amount of lateral support present to delay buckling of the fibres under compression loads is reduced

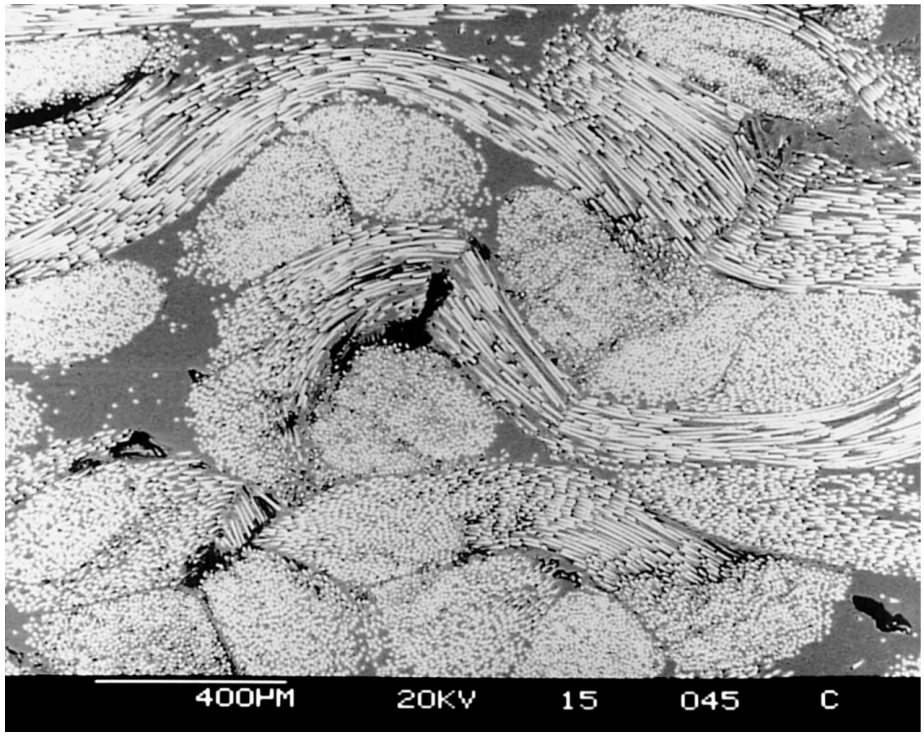

Figure 13 Scanning electron micrograph of a fibre failure in the knitted composites due to compression loading.

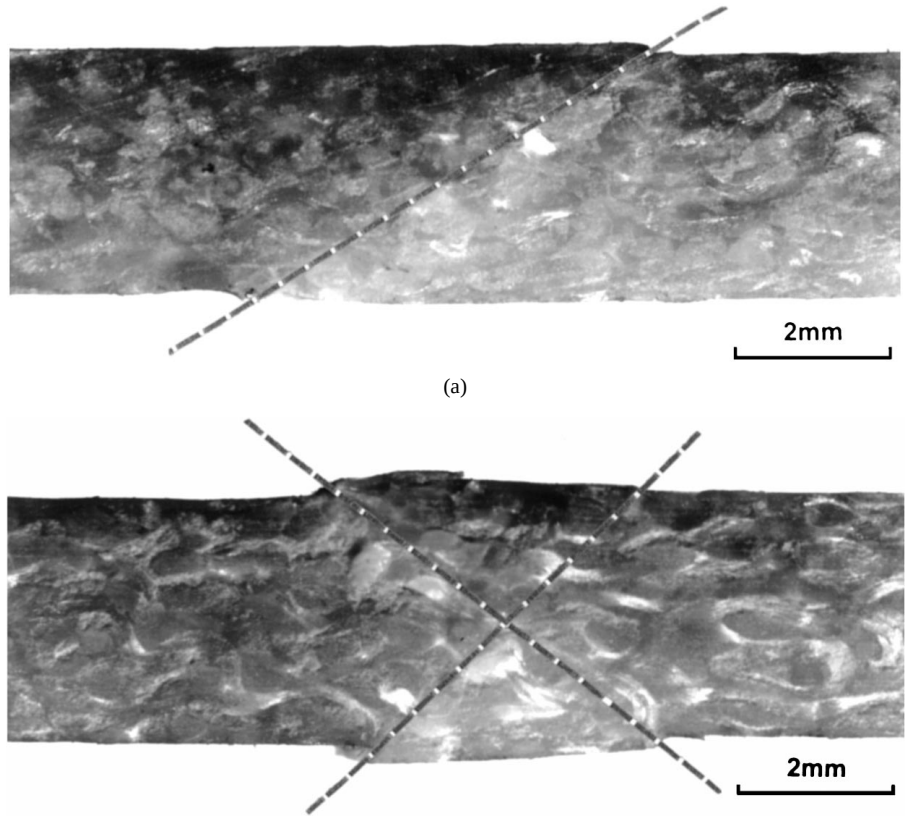

Figure 14 Representative compression failure. (a) shear (20CW). (b) shear-crush (45CW).

thereby bringing about a degradation in the compression strength.

Macroscopically, the laminates exhibit compressive failure by shear. There is strong evidence to suggest that in the present laminates shear failure initiates at one edge of the sample which then grows and propagates across the width of the sample as loading progresses. When a significant part of the sample has failed and the fracture surfaces have sheared cleanly over each other, the remainder of the sample collapses under the pressure of an excess load thus causing the far edge of the sample to be crushed. This failure sequence which

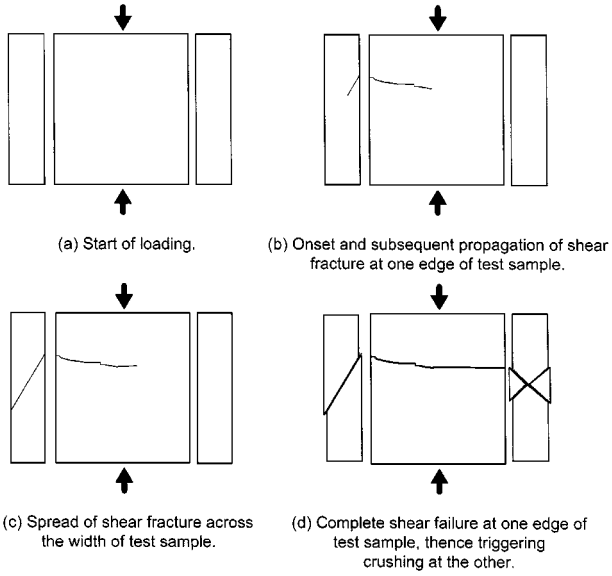

Figure 15 Schematic drawing depicting the series of events occurring during compression loading with the onset of shear fracture, at on edge of the test sample, up to ultimate failure and crushing, at the far edge of the test sample. (a) Start of loading. (b) Onset and subsequent propagation of shear fracture at one edge of test sample. (c) Spread of shear fracture across the width of test sample. (d) Complete shear failure at one edge of test sample thence triggering crushing at the other.

is common for all the laminates under investigation is described schematically in Fig. 15.

Contrary to the case of compression loading, the amount of deformation in the knitted fabric has a profound influence on the tensile fracture mode of the laminates with respect to the relative orientation of the fracture plane and the loading axis (see Fig. 11). Based on the maximum stress criteria, the fracture mode of unidirectional composites changes from transverse to shear and then finally to longitudinal as the loading angle rotates from 90° through to 0°. If the knitted composite laminate can be assumed to contain a finite number of fibre components, each oriented at different angles to the loading axis, then it is plausible that, with stretching the fibre components become more and more preferentially oriented so that with the associated improvement in fibre directionality, the dominant fracture mode transforms from transverse to shear. Further work is underway to verify this proposed failure mechanism through detailed microscopy and fibre orientation measurements of the various laminates.

5. Conclusions

In the undeformed state, the weft-knit Milano rib composite is on the whole anisotropic in tension and isotropic in compression. Under the influence of wale deformation, the tensile properties are improved regardless of the loading axis, however, under course deformation they are improved along the course axis and degraded along the wale. For compressive properties, wale deformation improves both strength and stiffness in the two principal loading axes, however, course deformation improves stiffness but degrades strength irrespective of the loading direction. Deformation in the knitted fabric also affects the tensile fracture mode whereby increased deformation, be it wale- or course-wise, transforms transverse fracture to shear fracture in either loading axis. On the contrary, the compressive fracture mode is insensitive to fabric deformation. Fractographic studies using stereo-optical and scanning electron microscopy have further revealed that tensile failure is caused by fibre breakages occuring at two locations of the knitted loops—one, at the leg components and, two, at fibre crossover points, whilst compression failure is controlled by Euler buckling of the looped fibres of the knitted composite. All these characteristics can be related back to the microstructure of the knitted composite laminates.

This study, therefore, highlights the fact that a knitted composite component is likely to contain soft spots and hard points that are caused by a change in knit structure due purely to stretching of the fabric during preforming. Whether these effects are relieved or compounded with stretching in more than one direction is still under investigation. Whilst shape knitting could minimise the need to stretch the knitted fabric during preforming, most near-net-shape knitted preforms are currently produced by altering the stitch density and/or knit architecture at selected locations of the preform which essentially means the absence of a uniform knit structure throughout the preform. Research into these issues is also continuing at the CRC-ACS (see for example [10]).

Acknowledgements

The authors are grateful to Dr A. P. Mouritz of the Defence Science and Technology Organisation (DSTO) for useful comments on the manuscript and help in arranging the microscopy sessions for this work. Thanks are also due to K. Houghton of CRC-ACS and M. Finch of RMIT for technical assistance in sample preparation and mechanical testing, respectively.

References

1. M. EPSTEIN and S. NURMI, in Proceedings of the 36th Intl. SAMPE Symp., April 1991, pp. 102–113.
2. S. RAZ, in "Proceedings of the 2nd TEXCOMP," edited by I. Verpoest and F. K. Ko (Leuven, Belgium, May 1994) p. 20.
3. B. QI, Private Communication, Cooperative Research Centre for Advanced Composite Structures Ltd (CRC-ACS), Bankstown, Australia, 1996.
4. I. VERPOEST and J. DENDAUW, in Proceedings of the 37th Int. SAMPE Symp. (Anaheim, CA, USA, March 1992) pp. 369–377.
5. S. W. HA, J. MAYER, J. DE HAAN, M. PETITMERMET and E. WINTERMANTEL, in "Proceedings of the 6th ECCM," edited by A. R. Bunsell, A. Kelly and A. Massiah (Bordeaux, France, September 1993) pp. 637–642.
6. M. NGUYEN, Final Year Project Dissertation, Royal Melbourne Institute of Technology, 1996.
7. K. H. LEONG, P. J. FALZON, M. K. BANNISTER and I. HERSZBERG, *Compos. Sci. Technol.* **58** (1998) 239.
8. S. RAMAKRISHNA and D. HULL, *ibid.* **50** (1994) 237.
9. W. L. WU, H. HAMADA, M. KOTAKI and Z. MAEKAWA, *J. Rein. Plast. Comp.* **14** (1995) 1032.
10. K. O. ANWAR, P. J. CALLUS, K. H. LEONG, J. I. CURISKIS and I. HERSZBERG, in "Proceedings of the 11th ICCM," Vol. 5, edited by M. L. Scott (Gold Coast, Australia, July 1997) pp. 328–340.

Received 19 June
and accepted 11 November 1998